Biochemistry and Biophysics Reports 27 (2021) 101089

Contents lists available at ScienceDirect

Biochemistry and Biophysics Reports

journal homepage: www.elsevier.com/locate/bbrep

SCLC-J1, a novel small cell lung cancer cell line

Kazuo Ohara [a], Shintaro Kinoshita [a], Jun Ando [a,b], Yoko Azusawa [b], Midori Ishii [a], Sakiko Harada [a], Yoichiro Mitsuishi [c], Tetsuhiko Asao [c], Ken Tajima [c], Taketsugu Yamamoto [d], Fumiyuki Takahashi [c], Norio Komatsu [a], Kazuhisa Takahashi [c], Miki Ando [a,e,*]

[a] Department of Hematology, Juntendo University School of Medicine, 2-1-1 Hongo, Bunkyo-ku, Tokyo, 113-8421, Japan
[b] Department of Transfusion Medicine and Stem Cell Regulation, Japan
[c] Department of Respiratory Medicine, Juntendo University School of Medicine, 2-1-1 Hongo, Bunkyo-ku, Tokyo, 113-8421, Japan
[d] Department of Thoracic Surgery, Yokohama Rosai Hospital, 3211, Kozukue, Kohoku-ku, Yokohama, Kanagawa, Japan
[e] Division of Stem Cell Therapy, Distinguished Professor Unit, The Institute of Medical Science, The University of Tokyo, 4-6-1 Shirokanedai, Minato-ku, Tokyo, 108-8639, Japan

ARTICLE INFO

Keywords:
B7-H3
DLL3
Established SCLC cell line
GD2
Small cell lung cancer
Somatic mutations

ABSTRACT

Small cell lung cancer (SCLC) is a type of high-grade neuroendocrine carcinoma. It initially responds to chemotherapy but rapidly becomes chemoresistant and it is highly proliferative. The prognosis in SCLC is poor. We have established a novel SCLC cell line, SCLC-J1, from a malignant pleural effusion in a patient with advanced SCLC. SCLC-J1 cells express ganglioside GD2, CD276, and Delta-like protein 3. *RB1* is lost.

These features of the new SCLC cell line may be useful in understanding the cellular and molecular biology of SCLC and in designing better treatment.

1. Introduction

Small cell lung cancer (SCLC) accounts for 15 % of all lung cancers [1]. It has an exceptionally high proliferative rate and metastasizes early [2] so that 80–85 % of patients present with extensive-stage disease on diagnosis [3]. While SCLC patients respond to initial chemotherapy, most relapse within 6 months, with median overall survival is about 10–13 months [4]; only 6–7% of patients with SCLC are alive 5 years after diagnosis [5,6]. SCLC is strongly linked to tobacco carcinogens, with 98 % of cases arising in current or former smokers [2,7]. Chromosomal rearrangements and a high mutation burden, including functional inactivation of 2 tumor suppressor genes, *TP53* and *RB1,* are frequent [2]. Furthermore, intratumoral heterogeneity of gene expression in SCLC leads to evolution from chemosensitivity to chemoresistance [8]. Although Immune-checkpoint inhibitors (ICI) have significantly improved outcomes for non-SCLC [9], ICI with etoposide plus platinum is effective in only a fraction of SCLC patients [4]. To improve prognosis in SCLC, we must better understand its cellular and molecular biology.

Toward this end, working from a malignant pleural effusion in a patient with advanced SCLC, we have established the cell line SCLC-J1. We describe its chromosomal complement and complexly abnormal karyotype, with harbored mutations, and its expressed-antigen profile in which heterogeneous gene expression marks coexisting subpopulations. The tumor-specific antigens ganglioside GD2, CD276, and Delta-like protein 3 (DLL-3) are expressed, whilst *RB1* is lost. Interrogation of SCLC-J1 has provided insights into SCLC biology that may permit better therapeutic targeting of tumor-specific antigens and minimizing intratumoral heterogeneity.

2. Materials and methods

2.1. Clinical findings

An asymptomatic 47-year-old Japanese man who had for 20 years daily smoked a pack of cigarettes in July 2018 underwent screening chest roentgenography. The left hilar contour was abnormal. Computerized tomography (CT) found a left upper lobe lung lesion with pleural thickening and widespread thoracic lymphadenopathy (Fig. 1A). Positron emission tomography confirmed these findings and demonstrated extensive bone involvement (Fig. 1B). Microscopy of a CT-guided needle biopsy of the lung mass found SCLC (Fig. 1C). The patient was referred to our hospital for further evaluation and treatment. In August 2018, a cisplatin plus irinotecan regimen was initiated (28-day cycle of cisplatin,

* Corresponding author. Department of Hematology, Juntendo University School of Medicine, 2-1-1 Hongo, Bunkyo-ku, Tokyo, 113-8421, Japan.
E-mail address: m-ando@juntendo.ac.jp (M. Ando).

https://doi.org/10.1016/j.bbrep.2021.101089
Received 4 June 2021; Received in revised form 16 July 2021; Accepted 22 July 2021

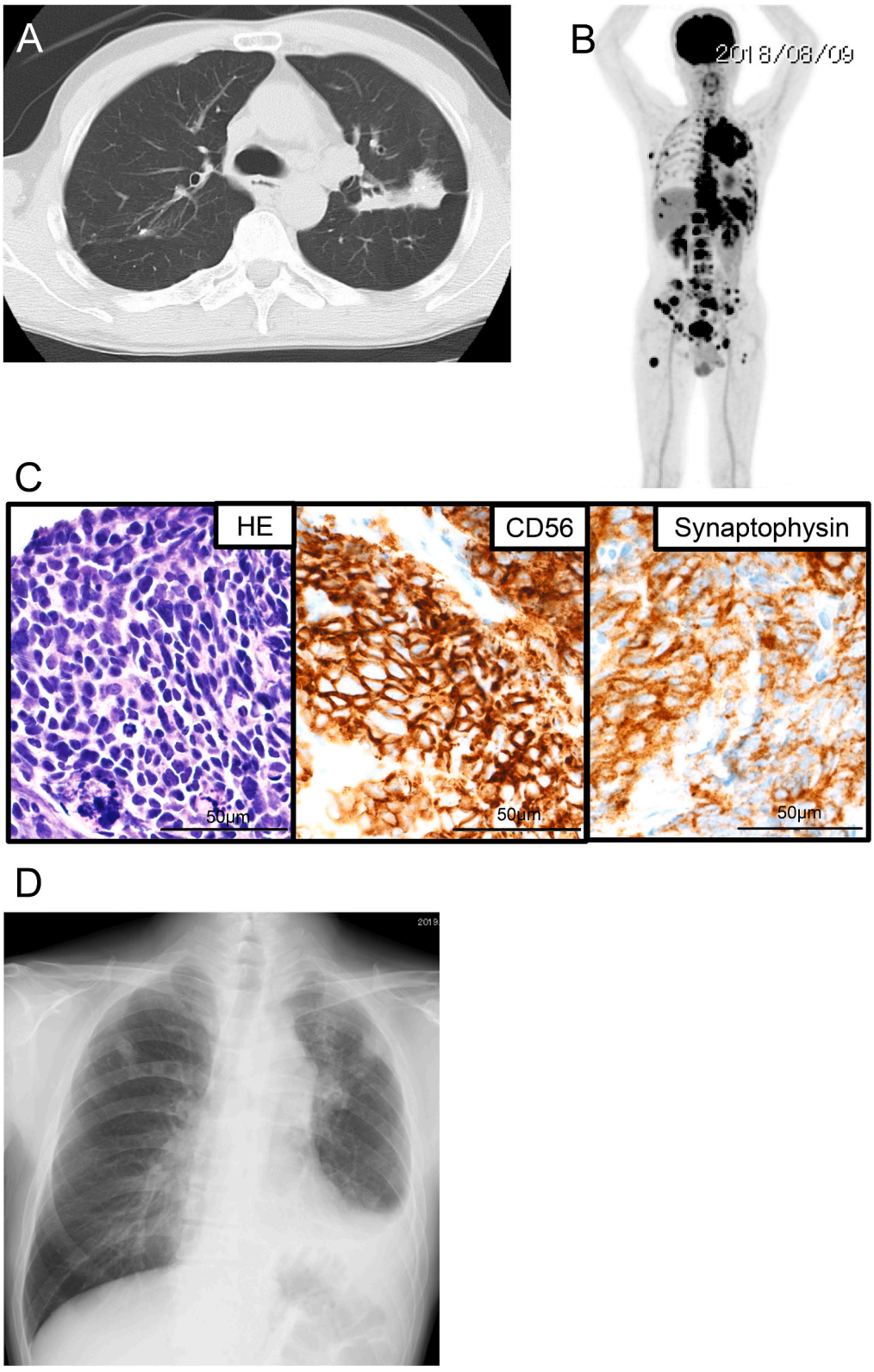

Fig. 1. Clinical and histopathological findings at presentation (A–C) and upon relapse (D). (A) 23-mm solid nodule, upper lobe, left lung, computerized-tomography (CT) image. A large mass (75 mm greatest dimension) encircles the ascending aorta, with lymph-node enlargement (bilateral supraclavicular, left axillary, subtracheal), left visceral pleural thickening, and scant left pleural effusion. (B) Widespread metastatic disease, positron emission tomography – CT image. Uptake is evident in the upper left lung, with a maximal standardized uptake value (SUV max) of 18.79, the left pulmonary hilus (SUV max 13.78), and the skeleton diffusely (SUV max 8.97–23.58). (C) Photomicrographs, lung needle biopsy specimen; all images original magnification 200x. Densely proliferated atypical cells with high nucleus: cytoplasm ratio (hematoxylin/eosin) on immunostaining expressed neural cell adhesion molecule (CD56) and synaptophysin. They did not express several leukocyte-associated antigens, the pan-cytokeratin AE1/AE3, the lung-adenocarcinoma marker thyroid transcription factor 1, or the squamous-cell carcinoma marker p40. (D) Left pleural effusion with mediastinal shift, chest roentgenogram, at relapse 7 months after presentation.

60 mg/m^2, on day 1, with irinotecan, 60 mg/m^2, on days 1, 8, and 15). However, disease progressed (Fig. 1D). Thoracentesis for palliation 7 months after presentation, with cytologic study of fluid, found SCLC. Amrubicin monotherapy (40 mg/m^2, every 3 weeks, on days 1 and 3) prolonged survival for 3 more months. Thereafter, at patient request, only end-of-life care was given, and death supervened.

2.2. Specimen collection and maintenance in culture

This study was approved by the Ethics Committee of Juntendo University and adhered to the tenets of the Declaration of Helsinki. Written informed consent was obtained from the patient. At thoracentesis, 500 ml of pleural fluid was collected in a sterile bottle. After 40 μm EASYstrainer filtration (Greiner, Kremsmünster, Austria), 50 ml was centrifuged and the supernatant was discarded. The pellet was then re-suspended in 5 ml of Roswell Park Memorial Institute 1640 medium (RPMI) (Thermo Fisher Scientific, Waltham, MA) supplemented with 10 % fetal bovine serum (FBS) (Gibco Life Technology, Carlsbad, CA) and 1 % penicillin/streptomycin/glutamine (PSG) (Thermo Fisher Scientific), transferred to a 25 cm^2 T25 tissue culture flask (TPP, Trasadingen, Switzerland) and incubated at 37 °C in room air supplemented with 5 % CO_2. The remaining pleural fluid was frozen for future analysis. Three days after, floating cells and adherent cells coexisted in the flask. Half of the supernatant (2.5 ml), with floating cells was removed, mixed with 1 ml of ACK erythrocyte lysing buffer (Lonza, Basel, Switzerland), and centrifuged. The pellet was re-suspended, washed twice in PBS (PH 7.4), mixed with 5 ml of RPMI supplemented with 10 % FBS and PSG, and placed in a new T25 flask for culture under the conditions described above (Passage 1). Tumor cells thereafter grew steadily with more than 90 % cell viability as assessed by trypan-blue dye exclusion testing.

We separately cultured floating cells and adherent cells in different T25 flasks from passage 2, with fresh media fed twice a week. When confluence was observed in adherent cells, half of the medium, with floating cells, was collected and centrifuged. the pelleted cells were seeded into a new T25 flask with 10 ml of fresh RPMI supplemented with 10 % FBS and PSG. Adherent cells were treated with 1 ml of 0.05 % trypsin-EDTA solution (Thermo Fisher Scientific) and seeded into a new T25 flasks in aliquots of half of the cells in 10 ml of fresh RPMI supplemented with 10 % FBS and PSG. Both the floating and the adherent cells proliferated stably in T25 flasks with >100 passages for more than 2 years, allowing us to infer that these cells were immortalized and constituted a cell line. We named the cell line SCLC-J1.

By phenotype, 2 sublines of SCLC-J1 existed, floating and attached; we hypothesized that these 2 cell subtypes were effectively the same. We assessed SCLC-J1 cells by flow cytometry, karyotyping, and immunostaining.

2.3. Calculation of growth rate

To determine the doubling time, 5×10^6/10 ml of SCLC-J1 floating cells were seeded into a new T25 flask, pipetted vigorously, and counted using a Bürker hemocytometer (Erma, Saitama, Japan). The trypan-blue dye exclusion test was used to determine cell viability. Cells were counted every 2 days for 2 weeks. The logarithmic portion of the growth curve was used to calculate the doubling time.

2.4. Cytogenetic analysis

Chromosomal G-band analysis of 50 metaphase SCLC-J1 floating cells was conducted using standard techniques (SRL, Tokyo, Japan).

2.5. Immunocytochemistry

Cultured floating cells at attached-cell confluence were collected from the flask, centrifuged, washed twice in PBS (pH 7.4) and fixed with 4 % paraformaldehyde for 4 h at room temperature. They again were washed in PBS, with centrifugation, and were transferred to 70 % ethanol, mechanically stabilized in agar, and as a pellet processed into paraffin. Sections at 4–5 μm were routinely stained with hematoxylin and eosin and immunostained (Ventana BenchMark GX, Roche Diagnostics, Rotkreuz, Switzerland) using an anti-human ganglioside GD2 rabbit polyclonal antibody (1:50 dilution; #1963, Matreya, State College, PA) and biotin-conjugated secondary antibody with diaminobenzidine as chromogen (iVIEW DAB Detection Kit, Roche Diagnostics) and hematoxylin as counterstain. SCLC-J1 floating cells incubated with antibody diluent without secondary antibody served as negative control.

2.6. Antibodies

Allophycocyanin (APC)-conjugated anti-human GD2, phycoerythrin (PE)-conjugated anti-human CD56, APC-conjugated anti-human CD276, APC-conjugated anti-human programmed death ligand 1 (PD-L1), APC-conjugated anti-human HLA class I antigens (HLA-A, B, C) (all BD Biosciences, San Jose, CA) and PE-conjugated goat IgG anti-human DLL3 (R & D Systems, Minneapolis, MN) were used to label cells for flow cytometry.

2.7. Flow cytometry and analysis

Flow cytometry was carried out on BD FACSCallibur or BD LSRFortessa equipment (both BD Biosciences). The acquired data were analyzed with FlowJo software 10.5.3 (Tree Star, Ashland, OR). Propidium iodide was used to gate in live cells in all analyses. Isotypes were used to interpret all flow cytometry data.

2.8. Targeted deep sequencing and data analysis

To investigate the genomic characteristics of SCLC-J1 and if primary SCLC cells of the pleural effusion and the established cell line, SCLC-J1, differed genetically, we analyzed by target sequencing the primary cells, *i.e.*, cells frozen immediately after thoracocentesis, as well as both floating and adherent subtypes of SCLC-J1. *TP53* and *RB* were sequenced using an in-house panel for lung-cancer – associated genes. Primers for targeted sequencing were designed using Ion AmpliSeq software (Thermo Fisher Scientific). Overall library preparation was carried out using an Ion Chef System (Thermo Fisher Scientific) according to the manufacturer's instructions. Barcoded libraries were generated from 20 ng of DNA per sample using an Ion AmpliSeq Chef Solutions DL8 Kit (Thermo Fisher Scientific). Two premixed pools were used to generate the sequencing libraries. Clonal amplification of the libraries was carried out by emulsion PCR. Library concentration was determined using an Ion Library TaqMan Quantitation Kit (Thermo Fisher Scientific). Library aliquots were sequenced on an Ion S5 Sequencer using an Ion 540 Chip and an Ion 540 kit–Chef Kit (Thermo Fisher Scientific).

The sequenced data were processed on standard Ion Torrent Suite Software (Thermo Fisher Scientific). Raw signal data were measured using Torrent Suite version 4.0. (Thermo Fisher Scientific). The pipeline consisted of signaling processing, base calling, quality score assignment, read alignment to human genome 19 reference (hg19), mapping quality control, and coverage analysis. Single-nucleotide variants and indels (insertions and deletions) were annotated on the Ion Reporter Server System (Thermo Fisher Scientific).

The variants were assessed *in silico* for likely effects using DDIG-in software V.9/13/2020 [10] and PROVEAN protein program V.1.1.3 [11].

3. Results

3.1. Cell line established from pleural effusion at relapse

Adherent and floating cultured-cell sublines coexisted (Fig. 2A). These 2 sublines proliferated stably. By some criteria, a cell line can be considered established after >30 passages [12]. However, SCLC-J1 has been cultured for >100 passages. Cell viability of both the sublines have always been >90 %. Growth kinetics were assessed by cell counting, with results charted to permit calculation of the population doubling time (~64.5 h; Fig. 2B).

3.2. Complex chromosomal abnormalities, SCLC-J1 cells

Various chromosomal abnormalities were detected in SCLC-J1 floating cells (Fig. 2C), with 37 (-Y, del [2](q?), der (3; 15) (q10; q10), der (6; 13) (p10; q10), −8, add (10) (p11.2), −12, −13, add (14) (p11.2), −15, −16, add (17) (p11.2), −18, add (19) (p13), −20, der (20) t (1; 20) (q21; q13.1)ins (20; ?) (q13.1; ?), add (21) (p11.2), −22, +marker 1, +marker [29/50] most frequent (Fig. 2D).

3.3. Tumor-specific antigen expression, SCLC-J1 cells

We analyzed cell surface antigen expression patterns of both floating and adherent SCLC-J1 sublines. Flow cytometric analysis revealed that most cells expressed GD2 (floating 86.6 %, adherent 88.2 %), CD56 (floating 99.9 %, adherent 96.1 %), and CD276 (floating 80.4 %, adherent 85.9 %). Fewer cells expressed DLL-3 (floating 63.7 %, adherent 76.7 %) (Fig. 3A). SCLC-J1 cells expressed programmed-death ligand 1 (floating 17.9 %, adherent 12.9 %) and strongly expressed HLA class I antigens (floating 99.7 %, adherent 99.9 %) (Fig. 3A). Tumor-specific antigen expression did not differ substantially between floating and adherent SCLC-J1 cells (Fig. 3A).

A

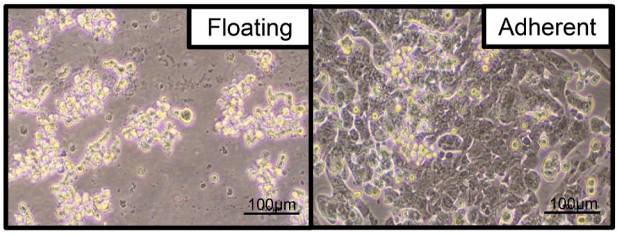

B

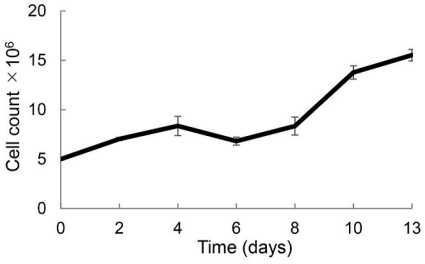

C

Chromosomal complement, SCLC-J1 cells	36	37	38	63	64	68	74	total
Number of cells per complement	2	29	5	2	10	1	1	50
Proportion	4%	58%	10%	4%	20%	2%	2%	100%
Karyotype, 37-chromosome variant	-Y, del(2)(q?), der(3;15)(q10;q10), der(6;13)(p10;q10), -8, add(10)(p11.2), -12, -13, add(14)(p11.2), -15, -16, add(17)(p11.2), -18, add(19)(p13), -20,der(20)t(1;20)(q21;q13.1)ins(20;?)(q13.1;?), add(21)(p11.2), -22, +marker1, +marker2							

D

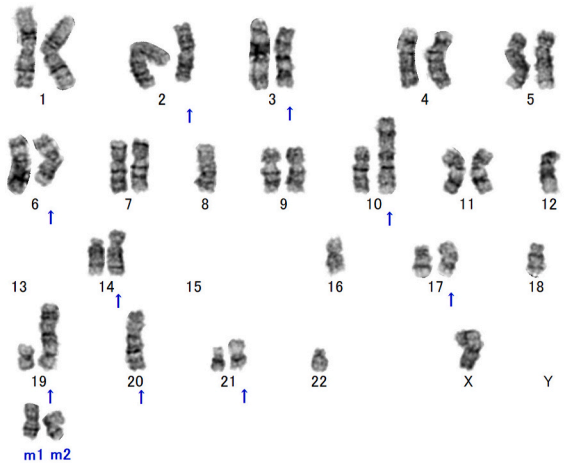

Fig. 2. Characterization of SCLC-J1 cells and cell line. (A) Phase-contrast light micrographs. Original magnification [x] 100. Inverted microscopy of floating and adherent subtypes of SCLC-J1 cells. (B) Proliferation curve of SCLC-J1 cells in culture. (C) Chromosomal counts, SCLC-J1 cells. Fifty cells in metaphase were evaluated. (D) Karyogram of most frequent complex chromosomal abnormalities detected in SCLC-J1 floating cells.

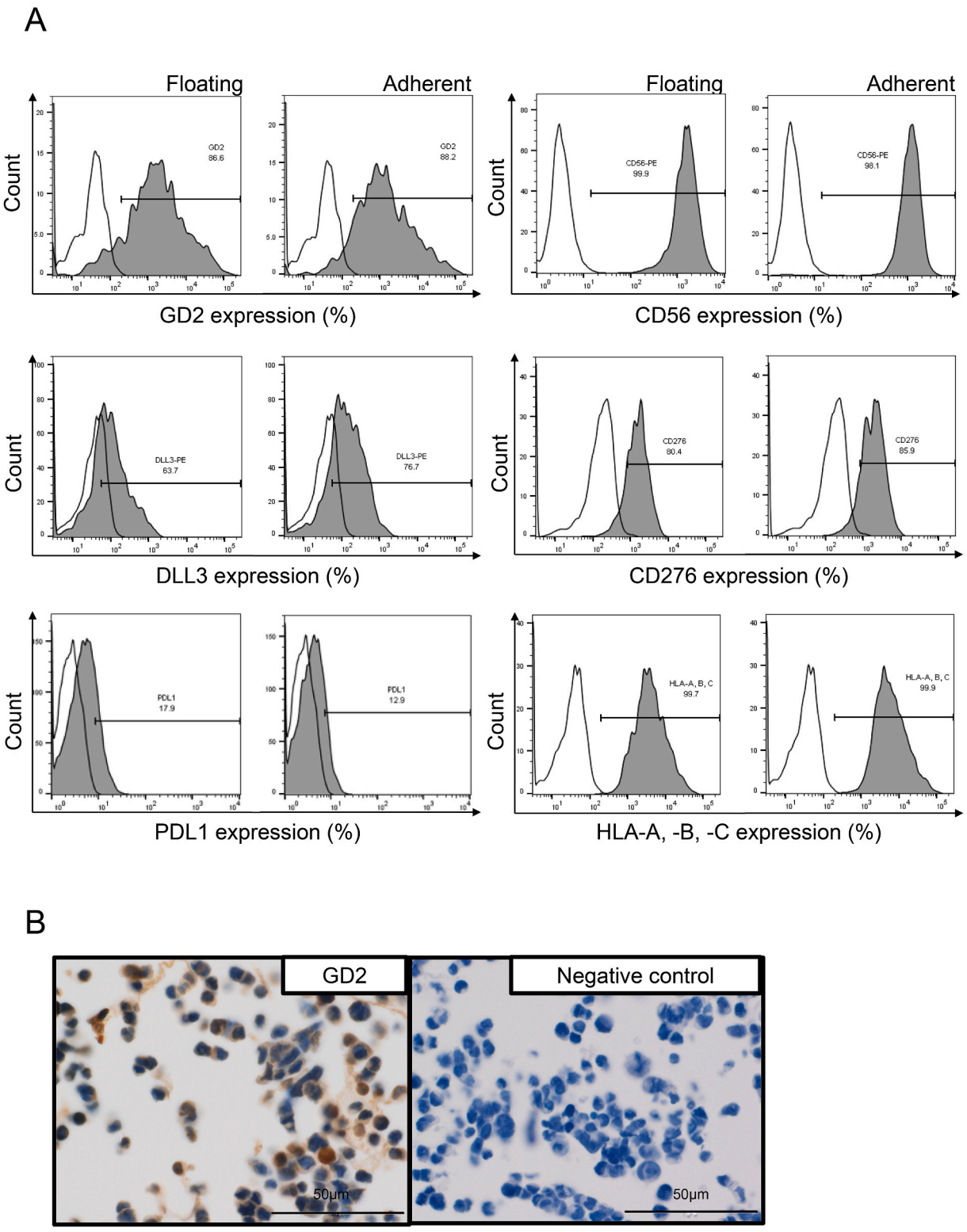

Fig. 3. Tumor-specific antigen expression on SCLC-J1 cells. (A) Floating and adherent subtypes of SCLC-J1 cells: Flow cytometric analysis of cell surface markers GD2, CD56, DLL3, CD276, PD-L1, and HLA-A, -B, and –C. (B) Immunocytochemical assessment, SCLC-J1 cells; *anti*-GD2 antibody.

3.4. SCLC-J1 cells express immunocytochemically demonstrable GD2

Immunocytochemical study of SCLC-J1 floating cells (Fig. 3B) showed that SCLC-J1 cells very closely resembled primary tumor cells on diagnosis (cf. Fig. 1C). Immunostaining also demonstrated GD2 expression by SCLC-J1 cells (Fig. 3B).

3.5. Targeted sequencing confirms RB1 mutation in SCLC-J1 cells

We confirmed that 99.75 % of SCLC-J1 adherent cells and 99.75 % of SCLC-J1 floating cells harbored the *RB1* mutation c.652 T > G (p. Leu218Val); 40.14 % of primary tumor cells harbored it (Table 1). No *TP53* mutation was observed in either primary cells or SCLC-J1 cells. In

Table 1
Somatic mutations in primary SCLC cells and SCLC-J1 detected by target sequencing.

Gene	Locus	% frequency			Type	Coding	Amino Acid Change	Variant Effect	DDIG-in	PROVEAN	SIFT
		Primary	Adherent	Floating							
RB1	chr13:48934197	40.14	99.75	99.75	SNV	c.652 T > G	p.Leu218Val	missense	NA	Neutral	Damaging
ARID1B	chr6:157502299	42.29	100	100	MNV	c.3332_3333delGGinsTT	p.Gly1111Val	missense	NA	Deleterious	Damaging
ARID2	chr12:46244712	66.27	99.52	99.57	SNV	c.2806G > T	p.Gly936Cys	missense	NA	Neutral	Damaging
SETD2	chr3:47155486	29.58	99.85	99.9	SNV	c.4595G > T	p.Arg1532Leu	missense	NA	Deleterious	Damaging
NF1	chr17:29657493	28.35	52.6	53.33	SNV	c.5789G > T	p.Cys1930Phe	missense	NA	Deleterious	Damaging
CDK6	chr7:92244492	21.18	20.96	28.07	SNV	c.943C > A	p.Pro315Thr	missense	NA	Neutral	Damaging
CDK4	chr12:58142975	6.72	5.99	12.22	SNV	c.809 A > T	p.Gln270Leu	missense	NA	Deleterious	Damaging
ARID1A	chr1:27106533	5.3	5.1	–	SNV	c.6144G > A	p.Trp2048Ter	nonsense	disease	NA	NA
ROS1	chr6:117622150	29.57	–	–	SNV	c.6720 T > G	p.Asn2240Lys	missense	NA	Neutral	Damaging
ROS1	chr6:117642495	30.63	–	–	SNV	c.5704G > A	p.Glu1902Lys	missense	NA	Neutral	Tolerated
POLE	chr12:133220098	5.27	–	–	INDEL	c.4337_4338delTG	p.Val1446fs	frameshift deletion	disease	NA	NA

primary cells, proportions harboring *ARID1B, ARID2, and SETD2* mutations were 42.29 %, 66.27 %, and 29.58 %, respectively (Table 1). After more than 100 passages, approximately 100 % of SCLC-J1 cells, in both adherent and floating sublines, harbored these mutations.

In silico analyses using PROVEAN and SIFT predicted deleterious effects for the variants identified in *RB1, ARID1B, ARID2, SETD2, NF1, CDK6*, and *CDK4* (Table 1).

4. Discussion

We successfully established a cell line, SCLC-J1, from pleural-effusion fluid in a patient with clinically advanced SCLC. On light microscopy of sections of an agar-embedded block of cultured cells, the cells resembled those sampled from lesional tissue at initial presentation.

In culture, SCLC-J1 cells formed floating clusters, a typical growth pattern of SCLC in liquid milieu [12]. Floating-subline cells grow as rounded clusters. They may die when dispersed into a single-cell suspension. This was reflected in reduced growth for a week after trypsin treatment and passage, with recovery thereafter. The population doubling time of this line (64.5 h) is similar to those of other reported SCLC cell lines [13].

Cytogenetic investigation of SCLC-J1 cells found a heterogenous population with complex karyotypes, consistent with the high tumor mutational burden known to characterize SCLC [14]. On this basis, one may expect that strong cytotoxic T cell responses can be induced against SCLC [5,15]. Immunotherapeutic approaches are thus proposed as effective for targeting tumor-specific antigens in SCLC [16]. We demonstrated that SCLC-J1 expresses the antigens GD2, DLL-3, and CD276. GD2 is a disialoganglioside specifically expressed on tumors from neuroectodermal origin, including SCLC. It reportedly has important roles in SCLC cell proliferation [17, 18]. It appears to participate in cell signaling but its function in normal cellular physiology has not been fully elucidated and understood [17]. It is considered a tumor-associated antigen and therefore is a valuable primary target for cancer immunotherapy. In several clinical trials, chimeric antigen receptor T (CART) cells directed against GD2 antigen were efficacious in high-risk neuroblastoma patients [19,20]. DLL3, a Notch ligand, inhibits activation of the Notch pathway [21]; it is directly regulated by achaetescute homolog-1, which is involved in pulmonary neuroendocrine cell development [22]. DLL3 is overexpressed on the cell surface in SCLC and other high-grade neuroendocrine tumors, whilst normal tissues have low expression or none [23]. DLL3-specific treatments for SCLC are being developed, such as antibody-drug conjugates [24], bispecific T cell engager immuno-oncology therapy [25] and CART therapy [26]. CD276 (B7–H3) is a type I transmembrane glycoprotein belonging to the immunoglobulin superfamily. The extracellular domain of human B7–H3 differs between its two isoforms, 4IgB7-H3 and 2IgB7-H3 [27]. B7–H3 is expressed on the cell surface in various solid tumors [28,29], including SCLC [30]. Clinical trials of B7–H3 – directed therapies such as CART therapy against recurrent or refractory glioblastoma (NCT04077866) and pediatric glioma (NCT04185038) are under way [28]. Pre-clinical screening trials of such approaches using SCLC-J1 cells, which express all three of these target antigens, may be valuable.

Representative genes that exhibit somatic mutation in SCLC are *TP53* and *RB1*; ~90 % of SCLC cell lines harbor *TP53* mutation with or without mutation in *RB1* [31]. On cataloguing somatic mutations in SCLC-J1 cells, we identified an *RB1* mutation. The frequency of this *RB1* mutation rose from 40.14 % of tumor cells at presentation to 99.75 % of SCLC-J1 cells after many passages in culture (Table 1). Selection for *RB1*-mutated populations during culture appears likely. Target sequencing also revealed *ARID1A*, *ARID1B,* and *ARID2* mutations in SCLC-J1 cells (Table 1). These genes encode the subunits of the ATP-dependent chromatin remodeling complex [32]. This complex shifts and restructures nucleosomes, contributing to epigenetic regulation [33]. Other genes in SCLC frequently undergo epigenetic modification [2] and several therapeutic strategies have targeted these changes [2]. Enhancer of zeste homolog 2 (EZH2), a master regulator of transcription, affects DNA methylation via upregulation of DNA methyltransferases [34]. Loss of *RB1* is associated with increased expression of EZH2 in SCLC [35]. EZH2 is strongly expressed in most SCLC and a histone modification placed by EZH2 is related to multiple chemoresistance including resistance to cisplatin [36]. Inclusion of an EZH2 inhibitor with standard cytotoxic reagents may prevent development of chemotherapy resistance in SCLC [37]. The EZH2 inhibitor tazemetostat upregulated GD2 expression in several cancers [38]. Combination therapy using epigenetic modifiers and targeted molecular immunotherapy thus appears within reach.

We have established from a malignant pleural effusion and characterized in terms of growth properties, cytologic appearance with immunocytochemical expression of selected antigens, and somatic mutations a new SCLC cell line, SCLC-J1. This new cell line holds promise in exploring both immunologic and genetics-based treatment for clinically advanced SCLC.

Authors' contributions

K.O., S.K., J.A., and S.H. performed experiments. S.K., M.I., Y.M., and Y.A. wrote the manuscript. M.A. directed the study and wrote the manuscript. Y.M. performed target sequencing. T.A. and K.T. provided

clinical information. F.T., N.K., and K.T. provided scientific discussions. All authors have read and approved the manuscript.

Funding

This study was supported by a grant from JSPS/KAKENHI (19K07781), and a Grant-in-Aid for Special Research in Subsidies for ordinary expenses of private schools from The Promotion and Mutual Aid Corporation for Private Schools of Japan (2019-36, 30–52).

Declaration of competing interest

The authors declare that they have no known competing financial interests or personal relationships that could have appeared to influence the work reported in this paper.

Acknowledgements

Written informed consent was obtained from the patient for publication and accompanying images. We thank A.S. Knisely for critical reading of the manuscript. This work was carried out in part at the Intractable Disease Research Center, Juntendo University Graduate School of Medicine. These studies were supported by a grant from JSPS/KAKENHI (19K07781), and a Grant-in-Aid for Special Research in Subsidies for ordinary expenses of private schools from The Promotion and Mutual Aid Corporation for Private Schools of Japan (2019-36, 30–52).

References

[1] J.P. van Meerbeeck, D.A. Fennell, D.K. De Ruysscher, Small-cell lung cancer, Lancet 378 (9804) (2011) 1741–1755.
[2] C.M. Rudin, E. Brambilla, C. Faivre-Finn, J. Sage, Small-cell lung cancer, Nat Rev Dis Primers 7 (1) (2021) 3.
[3] G.R. Simon, H. Wagner, P. American College of Chest, Small cell lung cancer, Chest 123 (1 Suppl) (2003), 259S-71S.
[4] C.M. Rudin, J.T. Poirier, L.A. Byers, C. Dive, A. Dowlati, J. George, et al., Molecular subtypes of small cell lung cancer: a synthesis of human and mouse model data, Nat. Rev. Canc. 19 (5) (2019) 289–297.
[5] L. Paz-Ares, M. Dvorkin, Y. Chen, N. Reinmuth, K. Hotta, D. Trukhin, et al., Durvalumab plus platinum-etoposide versus platinum-etoposide in first-line treatment of extensive-stage small-cell lung cancer (CASPIAN): a randomised, controlled, open-label, phase 3 trial, Lancet 394 (10212) (2019) 1929–1939.
[6] M.C. Pietanza, L.A. Byers, J.D. Minna, C.M. Rudin, Small cell lung cancer: will recent progress lead to improved outcomes? Clin. Canc. Res. 21 (10) (2015) 2244–2255.
[7] A.M. Varghese, M.F. Zakowski, H.A. Yu, H.H. Won, G.J. Riely, L.M. Krug, et al., Small-cell lung cancers in patients who never smoked cigarettes, J. Thorac. Oncol. 9 (6) (2014) 892–896.
[8] C.A. Stewart, C.M. Gay, Y. Xi, S. Sivajothi, V. Sivakamasundari, J. Fujimoto, et al., Single-cell analyses reveal increased intratumoral heterogeneity after the onset of therapy resistance in small-cell lung cancer, Nat. Can. (Que.) 1 (2020) 423–436.
[9] A.M. Dingemans, L. Hendriks, Immune checkpoint inhibitors in non-small-cell lung cancer: key to long-term survival? Lancet Respir Med 7 (4) (2019) 291–292.
[10] L. Folkman, Y. Yang, Z. Li, B. Stantic, A. Sattar, M. Mort, et al., DDIG-in: detecting disease-causing genetic variations due to frameshifting indels and nonsense mutations employing sequence and structural properties at nucleotide and protein levels, Bioinformatics 31 (10) (2015) 1599–1606.
[11] Y. Choi, A.P. Chan, PROVEAN web server: a tool to predict the functional effect of amino acid substitutions and indels, Bioinformatics 31 (16) (2015) 2745–2747.
[12] T. Skirecki, G. Hoser, J. Domagala-Kulawik, J. Kawiak, Characterization of a new small cell lung cancer (SCLC) cell line STP54 derived from a metastatic bioptate of a combined type of SCLC with Non-SCLC component, Folia Histochem. Cytobiol. 47 (1) (2009) 111–115.
[13] D.N. Carney, A.F. Gazdar, G. Bepler, J.G. Guccion, P.J. Marangos, T.W. Moody, et al., Establishment and identification of small cell lung cancer cell lines having classic and variant features, Canc. Res. 45 (6) (1985) 2913–2923.
[14] L.B. Alexandrov, S. Nik-Zainal, D.C. Wedge, S.A. Aparicio, S. Behjati, A.V. Biankin, et al., Signatures of mutational processes in human cancer, Nature 500 (7463) (2013) 415–421.
[15] L. Horn, A.S. Mansfield, A. Szczęsna, L. Havel, M. Krzakowski, M.J. Hochmair, et al., First-line atezolizumab plus chemotherapy in extensive-stage small-cell lung cancer, N. Engl. J. Med. 379 (23) (2018) 2220–2229.
[16] W.T. Iams, J. Porter, L. Horn, Immunotherapeutic approaches for small-cell lung cancer, Nat. Rev. Clin. Oncol. 17 (5) (2020) 300–312.
[17] B. Nazha, C. Inal, T.K. Owonikoko, Disialoganglioside GD2 expression in solid tumors and role as a target for cancer therapy, Front Oncol 10 (2020) 1000.
[18] W.N. William Jr., B.S. Glisson, Novel strategies for the treatment of small-cell lung carcinoma, Nat. Rev. Clin. Oncol. 8 (10) (2011) 611–619.
[19] C.U. Louis, B. Savoldo, G. Dotti, M. Pule, E. Yvon, G.D. Myers, et al., Antitumor activity and long-term fate of chimeric antigen receptor-positive T cells in patients with neuroblastoma, Blood 118 (23) (2011) 6050–6056.
[20] A. Heczey, C.U. Louis, B. Savoldo, O. Dakhova, A. Durett, B. Grilley, et al., CAR T cells administered in combination with lymphodepletion and PD-1 inhibition to patients with neuroblastoma, Mol. Ther. 25 (9) (2017) 2214–2224.
[21] E. Ladi, J.T. Nichols, W. Ge, A. Miyamoto, C. Yao, L.T. Yang, et al., The divergent DSL ligand Dll3 does not activate Notch signaling but cell autonomously attenuates signaling induced by other DSL ligands, J. Cell Biol. 170 (6) (2005) 983–992.
[22] M. Borges, R.I. Linnoila, H.J. van de Velde, H. Chen, B.D. Nelkin, M. Mabry, et al., An achaete-scute homologue essential for neuroendocrine differentiation in the lung, Nature 386 (6627) (1997) 852–855.
[23] L.R. Saunders, A.J. Bankovich, W.C. Anderson, M.A. Aujay, S. Bheddah, K. Black, et al., A DLL3-targeted antibody-drug conjugate eradicates high-grade pulmonary neuroendocrine tumor-initiating cells in vivo, Sci. Transl. Med. 7 (302) (2015) 302ra136.
[24] C.M. Rudin, M.C. Pietanza, T.M. Bauer, N. Ready, D. Morgensztern, B.S. Glisson, et al., Rovalpituzumab tesirine, a DLL3-targeted antibody-drug conjugate, in recurrent small-cell lung cancer: a first-in-human, first-in-class, open-label, phase 1 study, Lancet Oncol. 18 (1) (2017) 42–51.
[25] M.J. Giffin, K. Cooke, E.K. Lobenhofer, J. Estrada, J. Zhan, P. Deegen, et al., AMG 757, a half-life extended, DLL3-targeted bispecific T-cell engager, shows high potency and sensitivity in preclinical models of small-cell lung cancer, Clin. Canc. Res. 27 (5) (2021) 1526–1537.
[26] D.H. Owen, M.J. Giffin, J.M. Bailis, M.D. Smit, D.P. Carbone, K. He, DLL3: an emerging target in small cell lung cancer, J. Hematol. Oncol. 12 (1) (2019), 61.
[27] P. Steinberger, O. Majdic, S.V. Derdak, K. Pfistershammer, S. Kirchberger, C. Klauser, et al., Molecular characterization of human 4Ig-B7-H3, a member of the B7 family with four Ig-like domains, J. Immunol. 172 (4) (2004) 2352–2359.
[28] F. Kontos, T. Michelakos, T. Kurokawa, A. Sadagopan, J.H. Schwab, C.R. Ferrone, et al., B7-H3: an attractive target for antibody-based immunotherapy, Clin. Canc. Res. 27 (5) (2021) 1227–1235.
[29] D. Nehama, N. Di Ianni, S. Musio, H. Du, M. Patane, B. Pollo, et al., B7-H3-redirected chimeric antigen receptor T cells target glioblastoma and neurospheres, EBioMedicine 47 (2019) 33–43.
[30] D. Carvajal-Hausdorf, M. Altan, V. Velcheti, S.N. Gettinger, R.S. Herbst, D.L. Rimm, et al., Expression and clinical significance of PD-L1, B7-H3, B7-H4 and TILs in human small cell lung Cancer (SCLC), J Immunother Cancer 7 (1) (2019) 65.
[31] J. George, J.S. Lim, S.J. Jang, Y. Cun, L. Ozretic, G. Kong, et al., Comprehensive genomic profiles of small cell lung cancer, Nature 524 (7563) (2015) 47–53.
[32] N. Mashtalir, A.R. D'Avino, B.C. Michel, J. Luo, J. Pan, J.E. Otto, et al., Modular organization and assembly of SWI/SNF family chromatin remodeling complexes, Cell 175 (5) (2018) 1272–1288 e20.
[33] C.R. Clapier, J. Iwasa, B.R. Cairns, C.L. Peterson, Mechanisms of action and regulation of ATP-dependent chromatin-remodelling complexes, Nat. Rev. Mol. Cell Biol. 18 (7) (2017) 407–422.
[34] A.F. Gazdar, P.A. Bunn, J.D. Minna, Small-cell lung cancer: what we know, what we need to know and the path forward, Nat. Rev. Canc. 17 (12) (2017) 765.
[35] B.P. Coe, K.L. Thu, S. Aviel-Ronen, E.A. Vucic, A.F. Gazdar, S. Lam, et al., Genomic deregulation of the E2F/Rb pathway leads to activation of the oncogene EZH2 in small cell lung cancer, PloS One 8 (8) (2013), e71670.
[36] E.E. Gardner, B.H. Lok, V.E. Schneeberger, P. Desmeules, L.A. Miles, P.K. Arnold, et al., Chemosensitive relapse in small cell lung cancer proceeds through an EZH2-SLFN11 axis, Canc. Cell 31 (2) (2017) 286–299.
[37] A.B. Schulze, G. Evers, A. Kerkhoff, M. Mohr, C. Schliemann, W.E. Berdel, et al., Future options of molecular-targeted therapy in small cell lung cancer, Cancers 11 (5) (2019).
[38] S. Kailayangiri, B. Altvater, S. Lesch, S. Balbach, C. Gottlich, J. Kuhnemundt, et al., EZH2 Inhibition in Ewing sarcoma upregulates GD2 expression for targeting with gene-modified T cells, Mol. Ther. 27 (5) (2019) 933–946.